

Fig. 2 Voltage drop contributions with current

$$I_D = I_S \left(\exp\left(\frac{qV}{kT}\right) + 1 \right) \quad (1)$$

$$V_j = \log\left(\frac{I_D}{I_S} + 1\right) \times (VF10 + VF11 \times V(T) + VF12 \times V(T)^2) \times 0.0257 \quad (2)$$

$$V_c = I(V2) \times (VF20 + VF21 \times V(T) + VF22 \times V(T)^2) \quad (3)$$

here VF10, VF11, VF12, VF20, VF21, and VF22 (see Table 1) are the coefficients of the interpolation polynomial of the curve (temperature-dependent forward voltage drop) provided by the manufacturer.

2. The Leakage Current in Reverse

It is well known that modeling the reverse bias leakage current and breakdown voltage has evoked much attention in power electronic literature such as in Mantooth for example [16] where five reverse bias effects were added to the saturation current of the diode in Saber platform; while Maxim [17] proposed in turn a model based on the physics of semiconductor, with SPICE ABM blocks, including the reverse bias leakage current and avalanche effects.

The effects of leakage current and breakdown voltage may be either significant or otherwise in accordance with the voltage and power levels of the converter. In cases when one of these characteristics is insignificant, the model can be further simplified (by reducing complexity and the time of simulation).

However; if the leakage current vastly contributes to dissipation then it can be modeled by G2 which is an ABM source current controlled by an equation determined on the basis of the manufacturer's data. The control equation of the G2 is:

$$IR = (Eq1) \times \left(\frac{V(A)^2}{Eq2} \right)^{Eq3} \quad (4)$$

$$Eq1 = IR10 + IR11 \times V(T) + IR12 \times V(T)^2$$

$$Eq2 = IR20 + IR21 \times V(T) + IR22 \times V(T)^2$$

$$Eq3 = IR30 + IR31 \times V(T) + IR32 \times V(T)^2$$

The above IR10, IR11, IR12, IR20, IR21, F22, IR30, IR31, and IR32 are the coefficients of the interpolation polynomial

of the curve (reverse bias leakage current as a function of temperature) given by the manufacturer.

3. The Reverse Bias

The reverse recovery phenomenon takes place when a negative voltage is applied to the terminals of a conductive diode, yielding up the curves shown in Fig. 3. The curve of the current is split into three phases [18]:

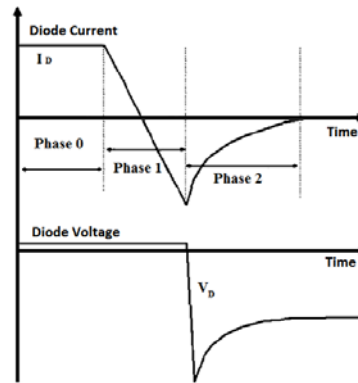


Fig. 3 The three phases of reverse recovery

Phase 0: ends when the diode begins to turn off.

Phase 1: is the charge storing stage during which excessive charges in the P region evacuated out. The charge control equation for minority carriers in the turn-off process is written as follows:

$$\frac{dQ(t)}{dt} + \frac{Q(t)}{\tau_F} = -i_n(0,t) = -i(t) \quad (5)$$

If we consider the current through the depletion capacity as well, (5) can be rewritten as follows:

$$\frac{dQ(t)}{dt} + \frac{Q(t)}{\tau_F} - C_{jn} \frac{dv(t)}{dt} = -i(t) \quad (6)$$

Phase 2: During this phase, the control and variation of the charge are non-linear (see Fig. 3), and in this case, the latter is described by (7) [17].

$$|Q(t)| = |i(t) \cdot \tau_R| \quad (7)$$

The current through C_{jn} cannot be overlooked since a junction voltage is about to be generated. So we use (6) as a charge control equation.

By applying this reasoning to our model:

It follows that the turn-off of the diode starts when the switch S1 is turned on and results in the G1 current flow through the R1-C1 circuit (Fig. 1). The E2 source (VCVS) controlled by a voltage V(60) across C1, generates at its output a voltage V(70), which is the control voltage source E3 (VCVS). Initially, this voltage (V(70)) has a negative value which allows a linear storage of the charges in the capacitor C3 (5). As soon as the voltage E3 (8) becomes positive, reverse recovery phase (phase 2) starts and instigates removal

of C3 charges through the R2 resistor. Once V (E3) reaches its maximum value, the capacitor C2 obtains the same potential across its terminals; Then the I(V1) current vanishes, cancels G1 input and sets its output current to 0 value, so that the output voltages of E2 and E3 sources automatically reaches zero (Fig. 1).

$$V = V(70) \times (QR10 + QR11 \times V(70) + QR12 \times V(70)^2) \quad (8)$$

QR10, QR11, and QR12 are the coefficients of the interpolation polynomial of the curve (variation of the C capacitor as a function of Vrev reverse voltage) given by the manufacturer.

B. The Thermal Part Model

The thermal impedance provided by the manufacturer's datasheet represents the instantaneous increase in the junction temperature of the device as a function of time [19]. It is represented by the RC pair of cells [20]-[23], and is dependent on the size of the semiconductor, the number and type of layers between the semiconductor and its case, and also the electrical insulation material. For our model we used 5 cells RC parallel.

The values of Ri and Ci are derived from the datasheet curve [19], [25]-[28], and calculated depending on Zth values (column Y) and τ_i (column X) for each n RC pairs according to (9).

$$Z_{th}(t) = \sum_{i=1}^n R_i \left(1 - \exp\left(-\frac{t}{\tau_i}\right) \right) \quad (9)$$

We first determine ZThmax maximum value (in permanent state), and then the approximate values of the first pole position which are defined by ZTh and its corresponding τ (x-axis) (10). The remained values of Rn and τ_n are respectively determined according to (11) and (12).

$$Z_{Th} = 0.7 \times Z_{Thmax} \quad (10)$$

$$R_n = R_1 \times 0.5^n \quad (11)$$

$$\tau_n = \frac{\tau_1}{n} (0.1^{n-1}) \quad (12)$$

We use the Simulated Annealing (SA) [24], technique to browse randomly (starting from an initialization) the pair values Zth and τ . Then, we compare the error of the current iteration with the best error formerly found. The latter is calculated by the least squares (LS) method for each time step (i) (13).

$$\text{Erreur} = \sum_1^i \left(\frac{R_\theta(i) - R_\theta(i)_{\text{best}}}{R_\theta(i)_{\text{best}}} \right)^2 \quad (13)$$

III. RESULTS

To assess the accuracy of the proposed model described in II, we performed simulations of some SiC MPS Diodes models (C3D04060E [19], CSD04060 [25], CSD10030 [26], SDP04S60 [27], SDP10S30 [28]), by using Orcad 16.6 Spice simulator. The values of model parameters obtained for all the tested devices are summarized in the below table as follows:

TABLE I
 THE CAPITALS, ASSETS AND REVENUE IN LISTED BANKS

	C3D04060E	CSD04060	CSD10030	SDP04S60	SDP10S30
Thermal Parameters					
TR1	2.432e-01	5.654e-01	5.838e-01	3.459e-02	1.450e-01
TR2	9.938e-01	1.353e+00	4.679e-01	6.801e-01	3.305e-01
TR TR3	1.211e+00	4.806e-01	7.535e-01	2.115e+00	9.898e-01
TR4	2.675e-01	7.073e-02	7.535e-01	1.613e-01	1.067e-01
TR5	4.541e-02	1.874e-02	2.107e-02	3.287e-01	1.816e-01
TC1	4.363e-01	5.609e-01	2.484e-01	6.597e+01	5.359e-01
TC2	1.890e-02	3.401e-03	2.955e-02	3.550e-02	4.597e-02
TC TC3	1.674e-03	8.970e-04	2.058e-03	1.230e-03	4.028e-03
TC4	1.671e-03	1.341e-04	4.246e-04	2.679e-04	1.141e-03
TC5	1.337e-03	3.021e-05	4.309e-05	1.375e-08	2.031e-07
Forward Voltage Drop					
VF10	5.871e-01	8.862e-01	7.123e-01	8.659e-01	9.548e-01
VF11	9.642e-04	-8.151e-05	-1.721e-03	1.398e-04	-8.042e-04
VF12	-2.991e-06	-1.729e-06	5.297e-07	-2.238e-06	-6.598e-07
VF20	2.885e-01	2.957e-01	9.332e-02	3.963e-01	1.001e-01
VF21	-1.426e-03	-1.732e-03	-3.877e-04	-1.967e-03	-3.816e-04
VF22	2.847e-06	3.794e-06	8.559e-07	3.956e-06	6.596e-07
Reverse Bias Charge					
QR10	8.894e-03	7.124e-03	2.449e-03	1.331e-02	2.750e-03
QR11	4.072e-04	2.804e-04	2.166e-04	5.901e-04	2.178e-04
QR12	-1.223e-06	-4.905e-07	-6.314e-07	-6.917e-07	-5.722e-07
Reverse Bias Leakage Current					
IR10	9.452e+00	4.131e+00	9.443e+02	1.080e+03	-5.312e+03
IR11	-4.458e-02	-1.024e-02	-5.433e+00	-6.624e+00	1.179e+01
IR12	5.279e-05	1.499e-05	7.720e-03	1.011e-02	1.899e-02
IR20	-6.145e+01	3.139e+02	4.282e+02	8.983e+02	2.593e+03
IR21	5.100e+00	1.285e+00	5.984e-01	1.376e+00	-9.529e+00
IR22	-9.340e-03	-2.328e-03	-3.170e-03	-2.876e-03	1.403e-02
IR30	-1.070e+02	-8.821e+00	9.213e+00	6.234e+00	-2.737e+01
IR31	6.884e-01	1.222e-01	7.580e-02	-2.149e-02	1.679e-01
IR32	-9.643e-04	-1.824e-04	-2.087e-04	4.070e-05	-2.159e-04

The external environment is presented by a voltage source whose value is the ambient temperature (Fig. 1). This model is valid for the 2nd and 3rd generation SiC MPS diodes.

The simulation results showed excellent correspondence to the measured curves provided by the manufacturer's datasheets for all voltages and currents in both forward and reverse bias, and in a wide range of operating temperature. An example of the obtained results for the simulations of CSD04060 diode in forward and reverse bias is shown respectively in Figs. 4 and 5, and all the curves of these figures correspond to the 25°C, 75°C, 125°C and 150°C temperature values. The thermal impedance curve is shown in Fig. 6 and the reverse recovery charge in Fig. 7. All these curves are presented with error bars of 5%.

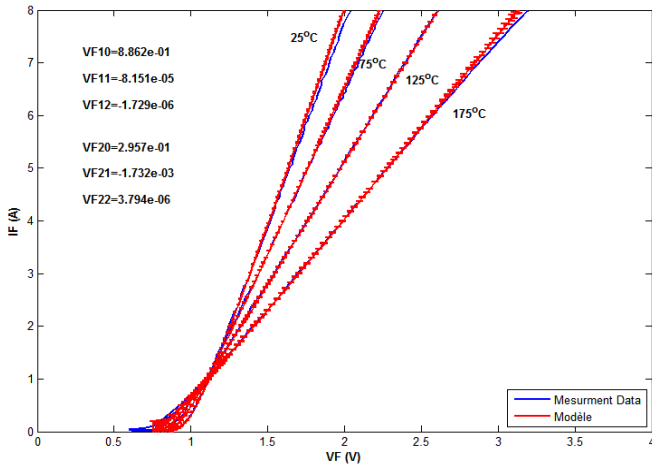


Fig. 4 Measured and simulated static forward characteristics of the CSD04060 MPS SiC diode

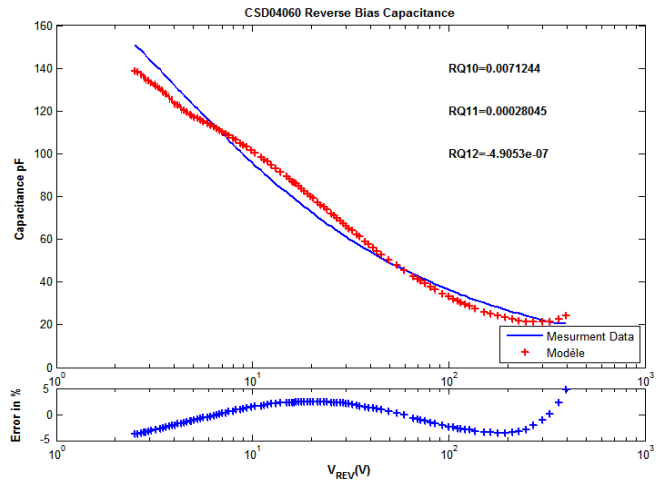


Fig. 7 Measured and simulated reverse recovery charge characteristics of the CSD04060 MPS SiC diode

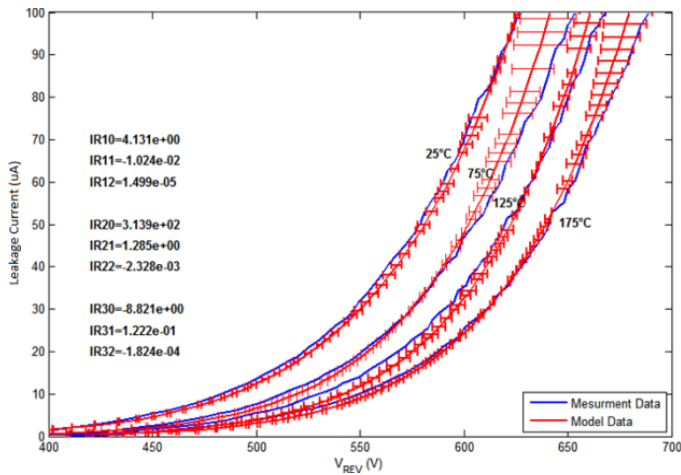


Fig. 5 Measured and simulated static reverse characteristics of the CSD04060 MPS SiC diode

The SiC MPS diode's (CSD04060) simulation of the dynamic behavior shown in Figs. 8 and 9 shows that the elimination of the stored charge starts when the voltage becomes negative. However; the final verification of the dynamic model has yet to be carried out in a cell of a switching power converter.

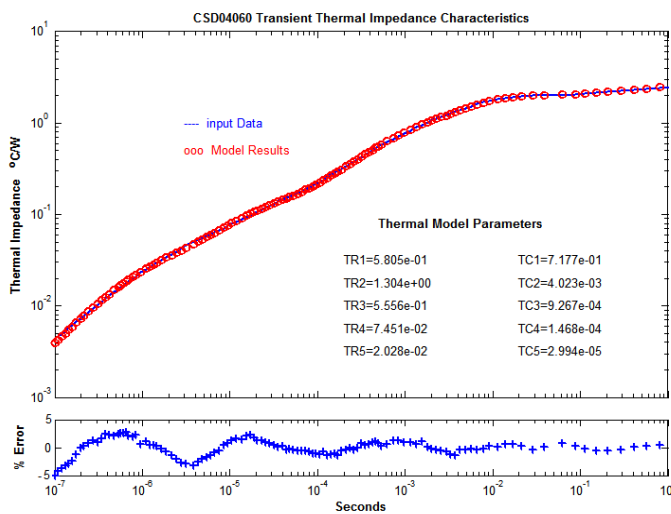


Fig. 6 Measured and simulated thermal impedance characteristics of the CSD04060 MPS SiC diode

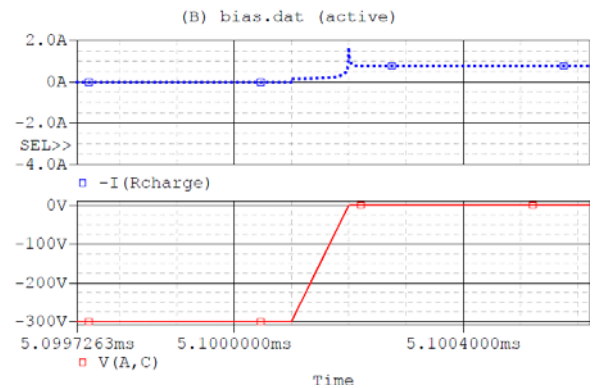


Fig. 8 Simulated dynamic behavior of the CSD04060 diode (turn-on)

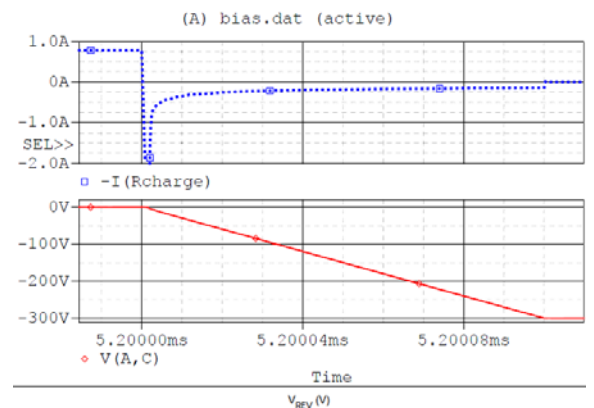


Fig. 9 Simulated dynamic behavior of the CSD04060 diode (turn-off)

IV. CONCLUSION

The proposed SiC MPS diodes behavioral electro-thermal model demonstrates excellent correspondence between the simulated forward and reverse bias and the curves provided by the devices' manufacturers. The estimation process of parameters which is based on two methods (i.e. weighted least square (WLS) and simulated annealing (SA)) has yielded satisfactory results. The basic advantage of the proposed model lies in its immanent simplicity and flexibility as to be implemented in modern simulators, adopting Spice programming (such as Berkeley SPICE, PSPICE).

REFERENCES

- [1] B.J. Baliga, "Analysis of a High-Voltage Merged p-i-n/Schottky (MPS) Rectifier". *IEEE Electron Device Letters*, Vol. EDL-8, No. 9. September 1987.
- [2] H.J. Hua, L.H. Liang, Z.Y. Ming, Z.Y. Men, T.X. Yan, C.F. Ping, and S.Q. Wen "Simulation study of a mixed terminal structure for 4H-SiC merged PiN/Schottky diode" *Chin. Phys. B Vol. 20, No. 11 (2011) 118401*.
- [3] S. M. Sze, and Kwok K. Ng "Physics of Semiconductor Devices" 3rd Edition A John Wiley & SONS 2007
- [4] B. J Baliga "Fundamentals of power semiconductor devices" Springer Science 2008.
- [5] J.S. Yuan and J.J. Liou "Semiconductor Device Physics and Simulation" Plenum Press 1998.
- [6] T.R. McNutt, A.R. Hefner Jr, H.A. Mantooth, J.L. Duliere, D.W. Berning, and R. Singh "Physics-based modeling and characterization for silicon carbide power diodes" *Science Direct, Solid-State Electronics Volume 50, Issue 3, March 2006, Pages 388–398*.
- [7] J. Dąbrowski, and J. Zarębski "Silicon Power Schottky Diodes Model Implemented in SPICE" *TCSET 2008, February 19-23, 2008, Lviv-Slavsko, Ukraine*.
- [8] F. N. Masana "SiC Schottky Diode Electrothermal Macromodel" *MIXDES 2010, 17th International Conference "Mixed Design of Integrated Circuits and Systems", June 24-26, 2010, Wroclaw, Poland*.
- [9] K.J. Tseng, C.F. Foo and P.R. Palmer "Implementing power diode models in Spice and Saber" 0-7803-1859-5/94/\$4.00 1994 IEEE.
- [10] G. L. Skibinski and W.A. Sethares "Thermal Parameter Estimation Using Recursive Identification" *IEEE Transactions on power electronics. Vol 6. No 2, April 1991*.
- [11] K. V. V. Murthy and R. E. Bedford "Transformation Between Foster and Cauer Equivalent Networks" *IEEE Transactions on Circuits and Systems, Vol. CAS -25, NO. 4, APRIL 1978*.
- [12] Star-Hspice Manual, Release 1998.2, July 1998.
- [13] Cadence OrCad, Help Product version 16.6 October 2012.
- [14] G. Massobrio, P. Antognetti, "Semiconductor Device Modeling with SPICE", 2nd edition, McGraw Hill, 1 December 1998.
- [15] J. Luo, K.J. Chung, H. Huang, and J.B. Bernstein, "Temperature dependence of Ron-sp in silicon carbide and GaAs Schottky diode" *IEEE 02CH37320. 40th Annual international Reliability Physics Symposium, Dallas. Texas, 2002*.
- [16] H. A Mantooth, Senior Member, IEEE, and Jeffrey L. Duliere "A Unified Diode Model for Circuit Simulation" *IEEE Transactions on Power Electronics, vol. 12, no. 5, September 1997*.
- [17] A. Maxim, D. Andreu, and J. Boucher, « A Unified High Accuracy SPICE Library For The Power Semiconductor Devices Built With The Analog Behavioral Macromodeling Technique" *ISPSO 2000. May 22-25. Toulouse, France*.
- [18] Y.C Liang, V.J Gosbell "Diode Forward and Reverse Recovery Model for Power Electronic SPICE Simulations" *IEEE Transactions on power electronics. Vol 5. No 3. July 1990*.
- [19] CSD04060–Silicon Carbide Schottky Diode, Datasheet, Rev. Q, Cree.
- [20] N. Jankovic, T. Ueta, K. Hamada, T. Nishijima, P. Igic "Unified Approach in Electro-Thermal Modelling of IGBTs and Power PiN Diodes" *Proceedings of the 19th International Symposium on Power Semiconductor Devices & ICs May 27-30, 2007 Jeju, Korea*.
- [21] A. Guerra, F. Vallone, "Electro-Thermal SPICE Schottky Diode Model Suitable Both at Room Temperature and at High Temperature," *International Rectifier, Dec. 1999*.
- [22] M. Marz, P. Nance, "Thermal Modeling of Power Electronic Systems," *Fraunhofer Institute, Apr. 2000*.
- [23] F.N. Masana "A straightforward analytical method for extraction of semiconductor device transient thermal parameters" *Microelectronics Reliability 47 (2007) 2122–2128 Science Direct Elsevier*.
- [24] R. Chibante "Simulated Annealing Theory with Applications" Published by Sciyo First published September 2010.
- [25] C3D04060E–Silicon Carbide Schottky Diode, Datasheet, Rev. E, Cree.
- [26] CSD10030–Silicon Carbide Schottky Diode, Datasheet, Rev. B, Cree.
- [27] SDP04S60 –Silicon Carbide Schottky Diode, Datasheet, Rev. 2.5, Infineon.
- [28] SDP10S30 –Silicon Carbide Schottky Diode, Datasheet, Rev. 1.5, Infineon.